The interacting effects of image acquisition date, number of images, classifier, and number of training samples on accuracy of binary classification of impervious cover

Article *in* Remote Sensing Letters · February 2018

DOI: 10.1080/2150704X.2017.1415478

CITATIONS
2

READS
172

2 authors:

Reza Khatami
University of Florida
15 PUBLICATIONS **478** CITATIONS
SEE PROFILE

Giorgos Mountrakis
State University of New York College of Environmental Science and Forestry
89 PUBLICATIONS **4,102** CITATIONS
SEE PROFILE

Remote Sensing Letters

ISSN: 2150-704X (Print) 2150-7058 (Online) Journal homepage: http://www.tandfonline.com/loi/trsl20

The interacting effects of image acquisition date, number of images, classifier, and number of training samples on accuracy of binary classification of impervious cover

Reza Khatami & Giorgos Mountrakis

To cite this article: Reza Khatami & Giorgos Mountrakis (2018) The interacting effects of image acquisition date, number of images, classifier, and number of training samples on accuracy of binary classification of impervious cover, Remote Sensing Letters, 9:2, 189-198, DOI: 10.1080/2150704X.2017.1415478

To link to this article: https://doi.org/10.1080/2150704X.2017.1415478

REMOTE SENSING LETTERS, 2018
VOL. 9, NO. 2, 189–198
https://doi.org/10.1080/2150704X.2017.1415478

Taylor & Francis
Taylor & Francis Group

The interacting effects of image acquisition date, number of images, classifier, and number of training samples on accuracy of binary classification of impervious cover

Reza Khatami[a,b] and Giorgos Mountrakis [b]

[a]Department of Geography, University of Florida, Gainesville, FL, USA; [b]Department of Environmental Resources Engineering, College of Environmental Science and Forestry, State University of New York, Syracuse, NY, USA

ABSTRACT

Selecting an appropriate time to acquire imagery for land-cover classification can have a substantial effect on classification accuracy. In this research, multi-temporal analysis of six Landsat images for binary impervious surface classification was conducted to investigate whether specific image dates (beyond simply leaf on/off) have a significant effect on impervious surface classification. We further examined the image date effects across training data sample sizes and classification algorithms. In terms of single time classification, the selection of an appropriate image time had the largest effect on the accuracy with a range of 7% to 10% between the most and least accurate classifications. The greenness transitional time between leaf off and leaf on (May images for our site) offered the highest performance. With multi-temporal images, an additional improvement in classification accuracy, up to 2.4%, was achieved when compared to the best single-time classification, when an advanced classifier (Support Vector Machine) was used. In addition, using all six available images with a reference data sample size as small as 150 pixels, classification accuracy was higher than that of many single-time classifications with substantially larger calibration data sample size. Our study suggests that there is considerable variability in classification accuracy of multi-temporal imagery and image dates should be carefully considered, beyond a general leaf on/off rule. Further testing should be conducted in other sites to identify optimal image dates.

ARTICLE HISTORY
Received 8 August 2017
Accepted 1 December 2017

1. Introduction

Urbanization typically results in an increase of impervious surface areas. Impervious surfaces, even though a small proportion of the entire earth surface, have substantial effect on urban ecology and climate. By extensive absorption and emittance of solar energy, impervious surfaces raise land surface temperature and can lead to formation of urban heat island (Haashemi et al. 2016). In addition, impervious surfaces, mainly consisted of waterproof materials, influence streamflow regime and water budget.

CONTACT Giorgos Mountrakis gmountrakis@esf.edu Department of Environmental Resources Engineering, College of Environmental Science and Forestry, State University of New York, 1 Forestry Drive, Syracuse, NY 13210, USA

Impervious surfaces increase surface water runoff that may cause an increase in flood frequency (Brun and Band 2000); cause thermal pollution of cold water ecosystems (Sabouri et al. 2013); and decrease of ground water recharge (Haase 2009). Moreover, by sealing of soil, impervious surfaces alter energy, water, and atmospheric gases exchanges, affecting numerous ecological functions of soil (Scalenghe and Marsan 2009). Consequently, impervious surface coverage is an important indicator for environmental studies.

Remote sensing images provide cost/time efficient means for environmental monitoring. A wide range of products is now available in regional to global scales (Grekousis, Mountrakis, and Kavouras 2015); satellite images are frequently used for impervious surface mapping (Yang et al. 2003; Yang et al. 2014; Khatami, Mountrakis, and Stehman 2017). Different categories of methods have been previously used for mapping of impervious surfaces using remote sensing images such as regression models (Okujeni et al. 2014); soft classification and spectral mixture analysis (Van de Voorde, De Roeck, and Canters 2009; Zhang et al. 2014); image hard classification (Luo and Mountrakis 2012); and fusion of remote sensing methods with urban growth models (Jin and Mountrakis 2013). In addition, previous studies introduced spectral indices that could be used for linking and mapping reflectance values to the impervious surfaces abundance. Examples of these indices are normalized difference impervious surface index (NDISI) (Xu 2010), modified NDISI (MNDISI) (Liu et al. 2013), and normalized difference built-up index (NDBI) (Zhou et al. 2014).

Considering the complexity of spatial patterns and substantial spectral reflectance variability of impervious surfaces, many studies used hyperspectral and high spatial resolution images for impervious area mapping. However, due to their global coverage, uneven revisit time interval, and low cost many studies used multispectral and medium resolution images for impervious mapping (Gong et al. 2013). Previous studies have shown that impervious surface mapping can benefit from integration of multi-temporal remote sensing images (Weng, Hu, and Liu 2009). Considering the approximately biweekly temporal resolution of Landsat, application of multi-temporal Landsat images is a common approach to compensate for its small number of bands for impervious surface mapping, for examples see: (McCauley and Goetz 2004; Henits, Jürgens, and Mucsi 2016). The underlying assumption is that the spectral signatures of some of the major classes such as vegetation, soil, and agriculture vary over time. These variations can be used as additional information, with respect to single-time image analysis, to improve mapping of impervious surfaces. Furthermore, for areas with frequent cloud cover such as tropical and coastal areas application of multi-temporal images is a solution to tackle cloud cover issue (Lu et al. 2008).

The objective of this study is to examine the effect of multi-temporal Landsat image selection for impervious surface mapping using hard classification methods. While, as mentioned, several studies exist looking at leaf on/off image combinations, our work is the first to look into specific dates in the leaf on/off transition and assess the value of each one on binary impervious surface classification. We further investigate the effects of two major factors including calibration data sample sizes, and classification algorithms. These factors have been previously identified as major approaches used to improve classification accuracy (Khatami, Mountrakis, and Stehman 2016). Results from this research provide a better understanding on the relative importance of those factors for impervious mapping accuracy improvement.

2. Materials and methods

2.1. *Dataset*

Our case study included the city of Syracuse and its surrounding neighborhood located in Central New York State, USA, an area of approximately 35 km × 27 km. All Landsat 5 Thematic Mapper (TM) images covering the case study area captured in the year 2000 with cloud cover smaller than 20% were used in this study. This included six Landsat 5 images acquired on 1 April, 24 April, 3 May, 20 June, 26 October, and 2 November in 2000 (the images from other dates, especially during winter, had considerable cloud coverage and were excluded from the analysis). In order to obtain fair comparisons among classifications of images from different dates only pixels that were cloud-free for all the six times were used in the analysis. In addition, during the classifications only the six reflective bands of Landsat images were used.

Reference data from previous work by Luo and Mountrakis (2010; 2011) was used in this study. To produce this reference data, high spatial resolution, 0.61 m pixel size, digital color-infrared aerial Emerge orthophotographs captured in 1999 were used to manually label Landsat pixels. The reference labels were created through manual interpretation of the orthophotographs overlaid on top of Landsat images. Reference labels were collected based on a two class classification scheme including impervious and pervious classes. During the manual reference data digitization, Landsat pixels that included any impervious pixels on the orthophotographs were assigned to the impervious class and all other pixels were assigned to the pervious class. The reason for applying this strategy instead of majority rule was to make sure all pixels with any impervious surface were identified. By doing so, the presented classification tasks can act as a precursor to a regression model for a continuous impervious surface product (percent imperviousness). The reference class labels were digitized for the entire 35 km × 27 km area, which means a census or complete coverage of reference data was available. Because Landsat images used in this study were captured within a seven-month period, the land cover was assumed to remain unchanged and the same reference data was used for classification of all images. Based on the reference labels, from all the cloud-free Landsat pixels, 216,799 belonged to the impervious class and 660,869 pixels belonged to the pervious class.

2.2. *Experimental design*

Our major objective was to investigate the effect of Landsat acquisition dates on the accuracy of impervious surface classifications. Starting with the imagery from six different dates in 2000, six single-time image classifications were performed. Moreover, a dual-time classification was implemented using all possible pairs of the six Landsat images resulting in fifteen dual-time classifications. Finally, one last classification was produced using all six Landsat images bringing the total number of classifications to 22 (6 single-time, 15 dual-time, 1 all-time). In every classification, all six reflective bands were included from the corresponding Landsat scene. Therefore, classification feature spaces for dual-time and all-time classifications include 12 and 36 bands, respectively.

Classification performance was investigated for different classification methods and varying calibration data sample sizes. Two popular classifiers including the k-nearest neighbor

(KNN) as a simple and intuitive algorithm, and the support vector machine (SVM) as a more advanced algorithm were chosen. In a meta-analysis of recent fifteen years of remote sensing image classification, Khatami, Mountrakis, and Stehman (2016) observed that SVM outperformed every other classifier and KNN, despite its simplicity, had larger accuracy than some of the main classifiers including Maximum Likelihood and Decision Tree.

Four data sample sizes including 150, 300, 1500, and 3000 sample pixels with equal number of pixels from each of the two classes randomly selected from the reference dataset were used for calibration of the classifiers. The calibration datasets were used to train and optimize the parameter values of the classifiers. For a given calibration dataset, two thirds of the sampled pixels selected at random, referred to as 'training dataset', were used to train the classifier based on different classifier parameter values. The remaining one third, referred to as 'optimization dataset', was used to test performance of the classifications based on different classifier parameter values to select the optimal values. Note that the accuracy assessment based on optimization dataset was conducted to optimize classifiers' parameter values and not to assess the accuracy of the final classified map products. Indeed, for accuracy assessment of the final map products and the results reported in this paper the reference data from the entire dataset was used, i.e., all the 877,668 pixels.

An optimization process was used to select the optimal parameter values of each of the classifiers by testing different parameter values. For KNN classifier, the only parameter optimized was K, the number of neighbors used for class assignment. Values from 1 to 20 were tested for optimal K identification. For the SVM classifier, the optimized parameters were penalty parameter and kernel width. The following values were tested for penalty parameter: 0.01, 0.1, 0.5, 1, 2, 5, 10, 25, 50, 100, and 300. Optimal kernel width was determined using MATLAB's heuristic search. For all SVM classifications a radial basis function (RBF) was used as the kernel function.

With respect to the accuracy assessment results reported in this manuscript, the average value of user's accuracy (UA) and producer's accuracy (PA) of the impervious class was used as accuracy measure; in the rest of the manuscript 'classification accuracy' refers to this measure. Because the focus of this study was on impervious surface mapping, the mentioned measure was used instead of overall accuracy. In addition, because optimization datasets were sampled using stratified random sampling, stratified estimators (Olofsson et al. 2014) were used for estimation of user's and producer's accuracies using the optimization datasets. For each classification, the parameter values that led to the largest classification accuracy were identified and the classification of the entire case study was done using the optimal parameter values. Finally, after the classification of the entire case study was done, the accuracy assessment of the classification was conducted by using the reference data from the entire case study.

The training, optimization and accuracy assessment processes were conducted independently for each set of the 22 combinations of multi-temporal images, the two classifiers, and the four calibration data sample sizes. This resulted in $22 \times 2 \times 4 = 176$ classifications. For each calibration data sample size, the same sampled calibration pixels were used for all classifications by the two classifiers and for all combinations of images. To account for variation in performance of classifications due to calibration data sampling variability, the process of calibration data sampling and classifications was repeated 10 times and the accuracy of each classification was averaged over the 10 repetition.

3. Results

Figure 1 shows the accuracy values, i.e. average of impervious class user's and producer's accuracies, for all sets of classifications. The first important observation is the variation of the classification accuracies among single-time classifications. For both classifiers and for all of the calibration data sample sizes single-time classification of images from May and November resulted in the highest and lowest accuracies, respectively. The differences between the accuracies of the most and least accurate single-time classifications range between 7% and 10%, for all different choices of classifier and calibration data sample sizes. As Table 1 shows, advantage of May image classifications over all other single single-time classifications were statistically significant. This indicates the importance of image date selection for impervious surface mapping as results can vary substantially. Moreover, as Table 1 (A) shows, improvements of May classifications over the other single-time classifications were statistically significant, except three cases.

In terms of the effect of multi-temporal images on classification accuracy, the two classifiers had different behavior. For the SVM classifier, all-time classification had the largest classification accuracy with a mean improvement in accuracy of 2.4% (averaged over the four calibration data sample sizes) with respect to the best single-time classification (also, improvements were statistically significant, see Table 1 (A)). For the dual-time classifications using the SVM classifier, many image combinations had larger accuracies than the best single-time classification, especially for the larger calibration data sample sizes, indicating the potential of multi-temporal image acquisition for improvement of impervious surface mapping. These improvements may not all be statistically significant though. On the other hand, for the KNN classifier, the accuracies of all-time and the most accurate dual-time classifications were either slightly higher than or comparable to the accuracies of the best single-time classifications. The largest improvements of multi-temporal classification with respect to the best single-time classification for the KNN classifier were obtained from dual-time classification of May image with either of the April images. The mean magnitude of this improvement, over

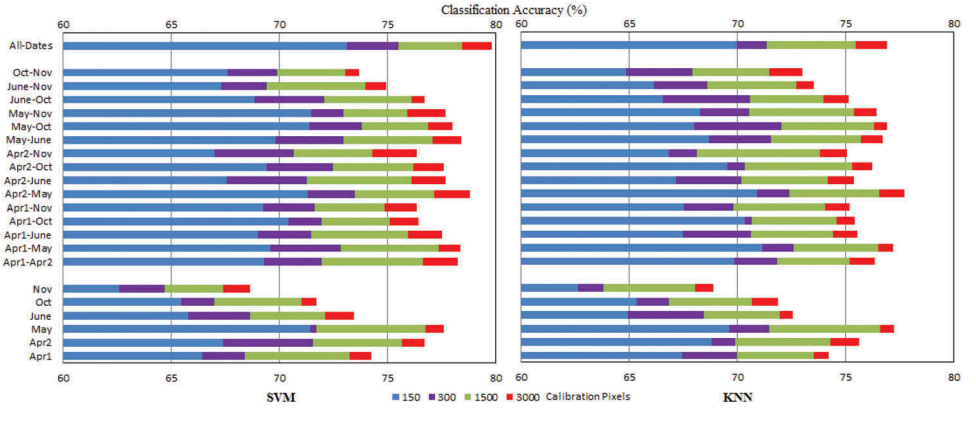

Figure 1. Cumulative classification accuracy for various choices of Landsat image dates, classification algorithms, and calibration data sample sizes. Classification accuracy is the average of UA and PA of the impervious class over 10 calibration dataset sampling repetitions over the entire reference dataset.

Table 1. Statistical tests (0.05 significant level) comparing classification accuracy of: (A) May (best single-time classification) versus all other image date combinations (RED: May accuracy was higher and statistically significant: GREEN: May accuracy was lower and statistically significant; WHITE: not significant); (B) All-time versus dual-time combinations (RED: Dual-time significant and greater than all-time; GREEN: Dual-time significant and smaller than all-time; WHITE: not significant).

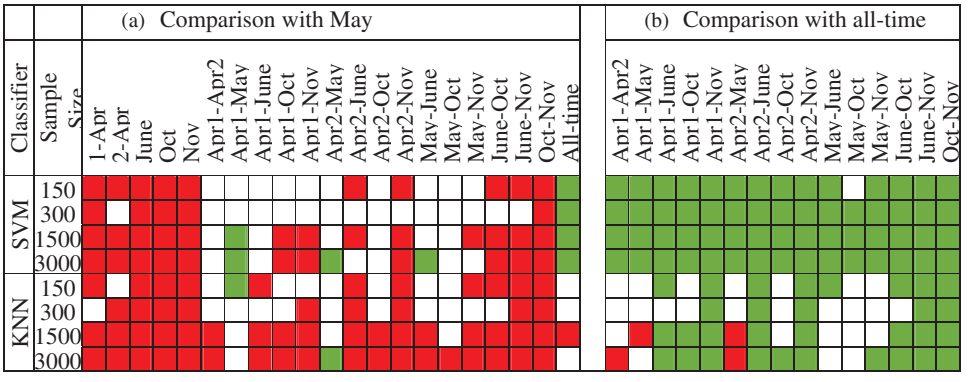

the four calibration data sample sizes, was 0.8%. Moreover, accuracy of all-time classification was larger than those of dual-time classifications for SVM classifier. However, for KNN classifier, the accuracy of all-time classification was even lower than those of some of the dual-time classifications (see Figure 1 and Table 1 (B)). Therefore, we conclude that multi-temporal information has the potential to increase classification accuracy; however, an advanced classifier should be employed to take advantage of the additional information contained in the input space.

Between the two classification algorithms, the SVM, as expected, outperformed the KNN. The advantage of the SVM over the KNN was larger for multi-temporal classifications when more images were used for classifications. While mean improvement, averaged over the four calibration sample sizes, in classification accuracy of the SVM over the KNN was only 0.2% for single-time classifications (mean over six single-time classification), the mean improvement increased to 1.2% and 3.3% for dual-time (mean over 15 dual-time classifications) and all-time classifications, respectively.

In terms of calibration data sample size, larger sample sizes improved classifications accuracy for all combinations of classifiers and images. However, increasing calibration data sample size was more effective when the initial calibration size was small. For example, increasing calibration data sample size from 150 pixels to 300 pixels (adding 150 pixels) on average (average over the 22 combinations of images) increased classification accuracy by 2.5% and 2.2% for the SVM and the KNN, respectively, while mean accuracy gain (average over the 22 combinations of images) was 1.3% and 1.0% for the SVM and the KNN, respectively, when increasing calibration sample size from 1500 pixels to 3000 pixels (adding 1500 pixels or an addition 10 times larger than the first case). We conclude that when the calibration data sample size is sufficiently large, the expected magnitude of improvement by adding more calibration data is small.

4. Discussion and conclusions

Spectral reflectance of the earth surface materials can change over time partially due to variations in their physical conditions. Examples include phenological changes in vegetation and seasonal variations in soil moisture. These temporal variations can change spectral reflectance separability of target classes. Consequently, land-cover image classification difficulty can vary at different times of the year and selecting an appropriate time to acquire the image used for land-cover classification can have substantial effect on classification accuracy. Moreover, image classification can benefit from application of multi-temporal images to improve the accuracy of resulting maps (Khatami, Mountrakis, and Stehman 2016).

In this research, we examined the potential of multi-temporal Landsat images for impervious surface mapping. Acquisition time had the largest effect on classification accuracy, up to about 10%, of single-time classifications, which indicates the importance of finding the best time of image acquisition. Generally, the image from May had the largest accuracy followed by the April images; the classification of the November image had the lowest accuracy. This finding follows a well-established observation, the substantial spectral confusion between soil and specific types of impervious surfaces (Luo and Mountrakis 2010). Our results indicate that using images in the early greenness stages (greening in our site typically occurs in late April) offers a good balance between enough vegetated ground coverage to separate soil and limited overhanging tree foliage that would confuse the impervious surface signature. This is further reflected on the normalized difference vegetation index (NDVI) summaries depicted in Figure 2. To create Figure 2, reference land-cover classes were manually digitized for 200 Landsat pixels using high-resolution images. The 200 reference pixels were collected for four classes of Hay/Pasture, Cultivated Crops, Deciduous Forest, and Impervious (50 reference pixels per class), which are the common land-cover classes in our site. The initial soil greening in Hay/Pasture class is affecting the last April and the May image. Note the significant greening increase in Deciduous Forest class in the June image that is also causing greening in the impervious class due to trees reaching over structures.

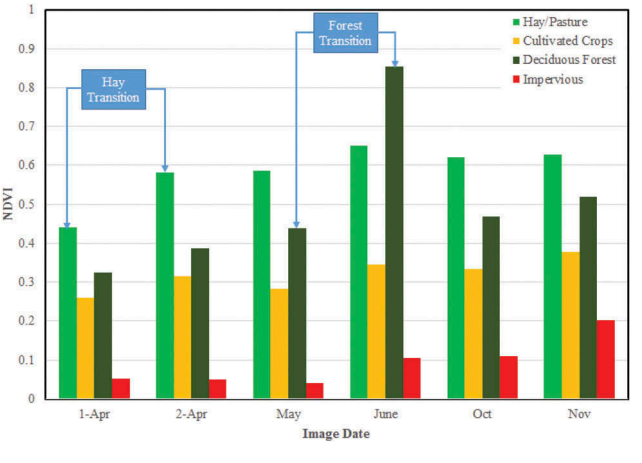

Figure 2. Averages of NDVI values for each Landsat image.

Overall, application of multi-temporal images improved classification accuracy by 2.4% on average, over the four calibration data sample sizes, with respect to the best single-time classifications when using an advanced classifier (SVM). Another conclusion is that to take advantage of the additional information contained in multi-temporal imagery a more complex classifier is needed. Our results indicate that the SVM classifier outperformed the KNN classifier, especially for multi-temporal classifications, with mean improvement of 3.3% (mean over the four calibration data sample sizes). Lastly, larger calibration data sample sizes improved classification accuracy, but with larger improvements when the initial calibration sample size was small.

The expected effect of classification factors is not equal. For example, acquisition time had up to approximately 10% effect on classification accuracy, which is more influential than classification algorithm selection. Moreover, interactions were observed between the effects of those factors. For instance, the improvement of SVM over KNN depended on whether a single-time or multi-temporal classification was conducted and varied from 0.2% for single-time classification to 3.3% for multi-temporal classification. Results from this research provide a better understanding on the relative importance of the investigated factors for impervious mapping accuracy improvement. This would help analysts to prioritize their efforts when trying to select a solution to improve their impervious surface mapping accuracy. For example, accuracy of the all-time classifications with a calibration data sample size as small as 150 pixels was larger than that of many single-time classifications with substantially larger calibration data sample size (Figure 1). Considering the free and easy availability of Landsat images, the application of multi-temporal images might be more straightforward, cost/time efficient, and practical than collecting more calibration data or implementing different classification algorithms.

While many factors affecting impervious surface mapping accuracy have been studied before, their interaction and relative importance requires further investigation. Here, as an initial work, relative importance of three of these factors are tested. However, it is important to test these factors on more images and areas for generalization of conclusions. Further research is necessary to examine other factors of impervious surface classification. Scene heterogeneity is another factor affecting the importance of image acquisition time. This research's study area is heterogeneous containing agriculture, urban/suburban, forested, and water land-cover/use. Therefore, image acquisition time had a major effect on classification accuracy. However, the image acquisition time might be less important if a case study is homogenous and different land-cover classes are spatially separated. Moreover, the optimal image acquisition times identified for the case study of this research can be different for the other regions with different greening periods. Further studies are required to examine the effects of those additional factors on impervious surface mapping.

Funding

This work was supported by the USDA Forest Service McIntire Stennis program, a SUNY ESF graduate assistantship and NASA's Land Cover Land Use Change Program (grant # NNX15AD42G).

ORCID

Giorgos Mountrakis http://orcid.org/0000-0001-5958-8134

References

Brun, S. E., and L. E. Band. 2000. "Simulating Runoff Behavior in an Urbanizing Watershed." *Computers, Environment and Urban Systems* 24 (1): 5–22. doi:10.1016/S0198-9715(99)00040-X.

Gong, P., J. Wang, L. Yu, Y. Zhao, Y. Zhao, L. Liang, Z. Niu, et al. 2013. "Finer Resolution Observation and Monitoring of Global Land Cover: First Mapping Results with Landsat TM and ETM+ Data." *International Journal of Remote Sensing* 34 (7): 2607–2654. doi:10.1080/01431161.2012.748992.

Grekousis, G., G. Mountrakis, and M. Kavouras. 2015. "An Overview of 21 Global and 43 Regional Land-Cover Mapping Products." *International Journal of Remote Sensing* 36 (21): 5309–5335. doi:10.1080/01431161.2015.1093195.

Haase, D. 2009. "Effects of Urbanisation on the Water Balance - A Long-Term Trajectory." *Environmental Impact Assessment Review* 29 (4): 211–219. doi:10.1016/j.eiar.2009.01.002.

Haashemi, S., Q. Weng, A. Darvishi, and S. K. Alavipanah. 2016. "Seasonal Variations of the Surface Urban Heat Island in a Semi-Arid City." *Remote Sensing* 8 (4): 352. doi:10.3390/rs8040352.

Henits, L., C. Jürgens, and L. Mucsi. 2016. "Seasonal Multitemporal Land-Cover Classification and Change Detection Analysis of Bochum, Germany, Using Multitemporal Landsat TM Data." *International Journal of Remote Sensing* 37 (15): 3439–3454. doi:10.1080/01431161.2015.1125558.

Jin, H., and G. Mountrakis. 2013. "Integration of Urban Growth Modelling Products with Image-Based Urban Change Analysis." *International Journal of Remote Sensing* 34 (15): 5468–5486. doi:10.1080/01431161.2013.791760.

Khatami, R., G. Mountrakis, and S. V. Stehman. 2016. "A Meta-Analysis of Remote Sensing Research on Supervised Pixel-Based Land-Cover Image Classification Processes: General Guidelines for Practitioners and Future Research." *Remote Sensing of Environment* 177: 89–100. doi:10.1016/j.rse.2016.02.028.

Khatami, R., G. Mountrakis, and S. V. Stehman. 2017. "Mapping Per-Pixel Predicted Accuracy of Classified Remote Sensing Images." *Remote Sensing of Environment* 191: 156–167. doi:10.1016/j.rse.2017.01.025.

Liu, C., Z. Shao, M. Chen, and H. Luo. 2013. "MNDISI: A Multi-Source Composition Index for Impervious Surface Area Estimation at the Individual City Scale." *Remote Sensing Letters* 4 (8): 803–812. doi:10.1080/2150704X.2013.798710.

Lu, D., H. Tian, G. Zhou, and H. Ge. 2008. "Regional Mapping of Human Settlements in Southeastern China with Multisensor Remotely Sensed Data." *Remote Sensing of Environment* 112 (9): 3668–3679. doi:10.1016/j.rse.2008.05.009.

Luo, L., and G. Mountrakis. 2010. "Integrating Intermediate Inputs from Partially Classified Images within a Hybrid Classification Framework: An Impervious Surface Estimation Example." *Remote Sensing of Environment* 114 (6): 1220–1229. doi:10.1016/j.rse.2010.01.008.

Luo, L., and G. Mountrakis. 2011. "Converting Local Spectral and Spatial Information from a Priori Classifiers into Contextual Knowledge for Impervious Surface Classification." *ISPRS Journal of Photogrammetry and Remote Sensing* 66 (5): 579–587. doi:10.1016/j.isprsjprs.2011.03.002.

Luo, L., and G. Mountrakis. 2012. "A Multiprocess Model of Adaptable Complexity for Impervious Surface Detection." *International Journal of Remote Sensing* 33 (2): 365–381. doi:10.1080/01431161.2010.532177.

McCauley, S., and S. J. Goetz. 2004. "Mapping Residential Density Patterns Using Multi-Temporal Landsat Data and a Decision-Tree Classifier." *International Journal of Remote Sensing* 25 (6): 1077–1094. doi:10.1080/0143116031000115102.

Okujeni, A., S. Van der Linden, B. Jakimow, A. Rabe, J. Verrelst, and P. Hostert. 2014. "A Comparison of Advanced Regression Algorithms for Quantifying Urban Land Cover." *Remote Sensing* 6 (7): 6324–6346. doi:10.3390/rs6076324.

Olofsson, P., G. M. Foody, M. Herold, S. V. Stehman, C. E. Woodcock, and M. A. Wulder. 2014. "Good Practices for Estimating Area and Assessing Accuracy of Land Change." *Remote Sensing of Environment* 148: 42–57. doi:10.1016/j.rse.2014.02.015.

Sabouri, F., B. Gharabaghi, A. A. Mahboubi, and E. A. McBean. 2013. "Impervious Surfaces and Sewer Pipe Effects on Stormwater Runoff Temperature." *Journal of Hydrology* 502: 10–17. doi:10.1016/j.jhydrol.2013.08.016.

Scalenghe, R., and F. A. Marsan. 2009. "The Anthropogenic Sealing of Soils in Urban Areas." *Landscape and Urban Planning* 90 (1–2): 1–10. doi:10.1016/j.landurbplan.2008.10.011.

Van de Voorde, T., T. De Roeck, and F. Canters. 2009. "A Comparison of Two Spectral Mixture Modelling Approaches for Impervious Surface Mapping in Urban Areas." *International Journal of Remote Sensing* 30 (18): 4785–4806. doi:10.1080/01431160802665918.

Weng, Q., X. Hu, and H. Liu. 2009. "Estimating Impervious Surfaces Using Linear Spectral Mixture Analysis with Multitemporal ASTER Images." *International Journal of Remote Sensing* 30 (18): 4807–4830. doi:10.1080/01431160802665926.

Xu, H. 2010. "Analysis of Impervious Surface and Its Impact on Urban Heat Environment Using the Normalized Difference Impervious Surface Index (NDISI)." *Photogrammetric Engineering & Remote Sensing* 76 (5): 557–565. doi:10.14358/PERS.76.5.557.

Yang, F., B. Matsushita, W. Yang, and T. Fukushima. 2014. "Mapping the Human Footprint from Satellite Measurements in Japan." *ISPRS Journal of Photogrammetry and Remote Sensing* 88: 80–90. doi:10.1016/j.isprsjprs.2013.11.020.

Yang, L., C. Huang, C. G. Homer, B. K. Wylie, and M. J. Coan. 2003. "An Approach for Mapping Large-Area Impervious Surfaces: Synergistic Use of Landsat-7 ETM+ and High Spatial Resolution Imagery." *Canadian Journal of Remote Sensing* 29 (2): 230–240. doi:10.5589/m02-098.

Zhang, C., H. Cooper, D. Selch, X. Meng, F. Qiu, S. W. Myint, C. Roberts, and Z. Xie. 2014. "Mapping Urban Land Cover Types Using Object-Based Multiple Endmember Spectral Mixture Analysis." *Remote Sensing Letters* 5 (6): 521–529. doi:10.1080/2150704X.2014.930197.

Zhou, Y., G. Yang, S. Wang, L. Wang, F. Wang, and X. Liu. 2014. "A New Index for Mapping Built-Up and Bare Land Areas from Landsat-8 OLI Data." *Remote Sensing Letters* 5 (10): 862–871. doi:10.1080/2150704X.2014.973996.